Infrared Difference Spectra of the Intermediates L, M, N, and O of the Bacteriorhodopsin Photoreaction Obtained by Time-Resolved Attenuated Total Reflection Spectroscopy

Christian Zscherp and Joachim Heberle*

Forschungszentrum Jülich GmbH, IBI-2: Structural Biology, 52425 Jülich, Germany

Received: March 24, 1997; In Final Form: July 10, 1997[⊗]

Attenuated total reflection spectroscopy, where precise control of external parameters is feasible, was combined with the step-scan technique, which provides time-resolved Fourier transform-infrared spectra with microsecond time resolution. The advantages of this new approach were demonstrated by analyzing the photoreaction of the membrane protein bacteriorhodopsin (BR). By variation of temperature and pH clear-cut separation of the intermediate states L, M, N, and O, was achieved while previous infrared studies failed to separate the O intermediate in the wild-type. Therefore, we focused on a detailed description of the O−BR difference spectrum. It was proved that the major changes in secondary structure of BR are reversed in the N to O transition. Bands at 1432 and 1448 cm^{-1} were tentatively assigned to CH_3 deformation vibrations of the retinal chromophore in the O state. At 1713 cm^{-1} the protonation of a carboxylic amino acid during the lifetime of O was observed. In addition to the wild-type data, the long-lived O intermediate of the E204Q and the E204T mutant have been investigated.

Introduction

Proton translocation in bacteriorhodopsin is initiated by absorption of visible light.[1,2] Several photointermediates (K, L, M, N, and O) can be distinguished in the visible as well as in the infrared spectral region. Infrared difference spectra between the intermediates and the initial unphotolyzed state deliver detailed information about the individual steps of proton translocation. Changes of the structure and environment of the chromophore as well as of the protein's secondary structure can be followed simultaneously. Even differences in the environment or the protonation state of single amino acids are observable.

After photon absorption the chromophore retinal, which is linked via a protonated Schiff base to K216, isomerizes from all-trans to 13-cis. In the L to M transition the Schiff base donates its proton to D85.[3] Concomitantly, another proton is released to the extracellular membrane surface.[4] E204 was suggested to be the release group based on theoretical[5] as well as on experimental[6] findings. In the M to N reaction the Schiff base is reprotonated by D96[7−9] while D85 is still protonated.[9] The subsequent proton uptake from the cytoplasmic side is kinetically optimized by surface-exposed carboxylic residues.[10] The infrared spectrum of the N intermediate shows the most prominent changes in secondary structure compared to the initial state.[11] From resonance Raman experiments it was concluded that reisomerization of retinal takes place during the N to O transition,[12] but reliable information about the protein in the O intermediate was missing. Two Fourier transform-infrared (FT-IR) investigations revealed conflicting results.[13,14] It is the kinetic degeneracy of the reset reaction sequence that makes the O intermediate notoriously resistant to clear separation from the other long-lived intermediates M and N.

With ATR (attenuated total reflection) spectroscopy recording of infrared spectra at well-defined pH and temperature is feasible. In combination with time-resolved techniques[15] we demonstrate that the intermediates of BR can be separated by selecting appropriate conditions. In particular, the ATR approach allows measurements at low pH and high temperature. By this means the transient concentration of O is increased. Conditions were selected where contributions from other intermediates are negligible. The resulting O−BR difference spectrum obtained from wild-type BR exhibits only minor bands in the amide I region excluding the occurrence of structural changes as large as those of the N intermediate. Bands specific for the O intermediate and not described before are tentatively assigned to antisymmetric CH_3 deformation vibrations of the chromophore retinal. They are a consequence of a distorted conformation of retinal in O. In the carbonyl region a band appears that corresponds to a carboxylic amino acid side chain which is protonated during or after O. In comparison, we present the O−BR difference spectrum of the mutants E204Q and E204T where a long-lived O intermediate exists. Good overall agreement between the mutants and wild-type O can be stated. Detailed analysis reveals that bands caused by changes in secondary structure are altered in the mutant as compared to the wild-type. These differences do not involve the amide I band at 1670 cm^{-1}, which loses most of its amplitude during the N to O transition.

Materials and Methods

Wild-type BR within the purple membrane (PM) was prepared from *Halobacterium salinarium* strain S9.[16] E204T and E204Q point mutants of BR were obtained as described.[10] For ATR spectroscopy 80 μL PM suspension (2.5 mg/mL) was slowly dried on a ZnS or ZnSe internal reflection element (IRE). After mounting the IRE into the ATR holder the sample was covered with 2 mL of a 1 M KCl, 25 mM buffer solution (citrate, phosphate, or carbonate for the respective pH). Samples were thermostated at 20 or 40 °C. After 2 h of swelling of the PM film the whole spectrometric setup was stable.

Time-resolved ATR/FT-IR spectroscopy was described in detail.[15] Briefly, FT-IR measurements were performed on a Bruker IFS 66v equipped with step-scan option and an "out-of-compartment" ATR accessory. For pulsed excitation a Nd:YAG laser was used (frequency-doubled output at 532 nm, pulse duration 8 ns, excitation energy 3 mJ/cm^2). Homogeneous illumination of the sample was achieved by a quartz fiber

* To whom correspondence should be addressed.

[⊗] Abstract published in *Advance ACS Abstracts,* November 15, 1997.

S1089-5647(97)01047-X CCC: $14.00

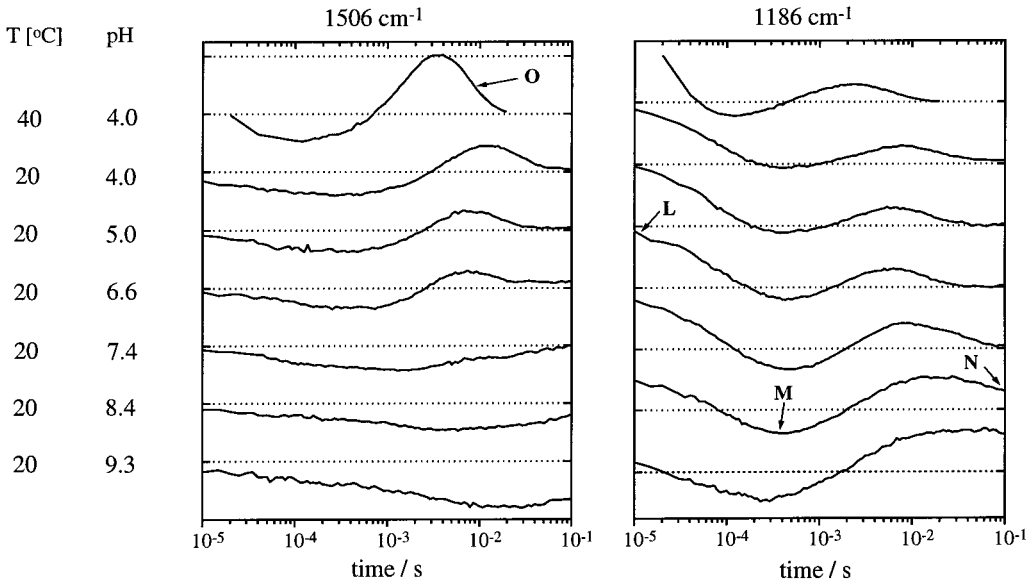

Figure 1. Time traces at 1506 and 1186 cm^{-1} extracted from time-resolved ATR/FT-IR measurements recorded at different pH and temperatures as displayed. Data sets from step-scan measurements under different conditions have been scaled to the same maximum amplitude at 1526 and 1200 cm^{-1}. Arrows indicate at which conditions (time, pH, temperature) intermediate spectra are taken (see Figure 2).

bundle. For measurements at pH 4 and 40 °C a digitization rate of 50 kHz was used. For the 20 °C time traces data digitized with 10 kHz were appended to 200 kHz data. A broadband interference filter (OCLI) limited the free spectral range from 1900 to 1000 cm^{-1}. Spectral resolution was 4.5 cm^{-1}. Between 5 and 20 measurements at each mirror position were averaged. Maximum repetition rate of the excitation laser was 6 Hz. Data resulting from measurements before and after laser excitation were processed by coadding of neighboring data points on a logarithmic time scale. To increase the number of reference spectra for the measurements with 10 kHz digitization rate a home-built 2 ms delay unit was inserted between the triggering aquisition processor of the FT-IR instrument and the Nd:YAG laser. Further improvement of the signal-to-noise ratio was achieved by averaging up to 25 of these difference spectra. To correct for a very small ($\Delta A < 4 \times 10^{-4}$) and rapidly decaying ($\tau = 20$ μs) frequency-independent offset artifact caused by laser-induced absorption changes of the IRE, a measurement with buffer only is subtracted. The O−BR difference spectra of the E204Q and the E204T mutant were recorded with the rapid-scan technique (4000 and 1200 averages, respectively). Applying the rapid-scan technique is appropiate because O decay is slowed by a factor of 10 in the E204Q mutant and 3-fold in E204T.

To reduce the number of data for global analysis, singular value decomposition[17] (SVD) as provided by Matlab software (The MathWorks, Inc.) was applied. SVD separates the matrix of the time-resolved data into time-dependent and spectral components of descending significance. In our case the linear combination of the first four components is sufficient for reproduction of the dataset. This was checked by the absence of any systematic undulations in the residuals. Thus, by simultaneous fitting of the first four time-dependent components, determination of the global rate constants is possible. Time traces were fitted with sums of exponentials as described.[18] It should be stressed, however, that the difference spectra shown are those actually measured. SVD treatment was only applied prior to fitting of (apparent) rate constants.

Results and Discussion

Separation of Intermediates. The combination of ATR with time-resolved difference spectroscopy allows observation of biomaterial in excess water. By variation of temperature and pH it is possible to separate the intermediates of the BR photoreaction.[19] This is demonstrated in Figure 1, where time traces at 1186 and 1506 cm^{-1} at different measuring conditions are shown. We selected these wavenumbers because at 1506 cm^{-1} bands of the C═C stretch vibration of the chromophore in the intermediates K (in the μs time domain) and O (ms) are absorbing; at 1186 cm^{-1} bands of C−C stretch vibrations of retinal in L (μs) and N (ms) are observable which are characteristic of a protonated 13-cis chromophore. M−BR does not show positive bands in this spectral region, whereas O−BR has a maximum at 1168 cm^{-1} with a shoulder at 1185 cm^{-1} (cf. Figure 2). A comparison of the time traces of Figure 1 shows that there is no contribution of the intermediate K (see traces at 1506 cm^{-1}) but a rapidly decaying L signal at early times which is larger at lower pH values. The 10 μs spectrum at 20 °C of pH 6.6 represents the L−BR difference spectrum. At high pH the rise of M is faster but the decay is slower than at low pH. Therefore, spectra between 0.3 and 0.4 ms at pH 8.4 have been averaged to compute the M−BR difference spectrum. At late times of the photoreaction at high pH a strong accumulation of N is observed. Consequently, the N−BR difference spectrum has been taken from spectra between 80 and 100 ms and pH 8.4. Separation of O is more difficult. Although at pH 4 and 40 °C a large absorption change at 1506 cm^{-1} is observed, there are still small contributions of M at 4 ms when O reaches its maximum concentration. We used data at pH 4.0 and 40 °C and averaged spectra between 5 and 10 ms to calculate the O−BR difference spectrum, i.e., at times when O has almost decayed. Bands characteristic for the N intermediate are negligible under these conditions. The O−BR difference spectrum in D_2O has been taken from data between 10 and 20 ms of a measurement at 40 °C and pD 4.4. The reason for the different times chosen for H_2O and D_2O is the kinetic isotope effect of O. By fitting the time trace at 1506 cm^{-1} as well as by global fitting of the data (at 40 °C) we determined the time constants for rise and decay of O in H_2O to be 1.9 and 3.8 ms, respectively. For the O kinetics in D_2O, the respective time constants are prolonged to 3.7 and 9.1 ms, which is in agreement with visible spectroscopy.[20] The larger kinetic H/D effect for the decay compared to the rise leads to a higher transient concentration of O in D_2O.

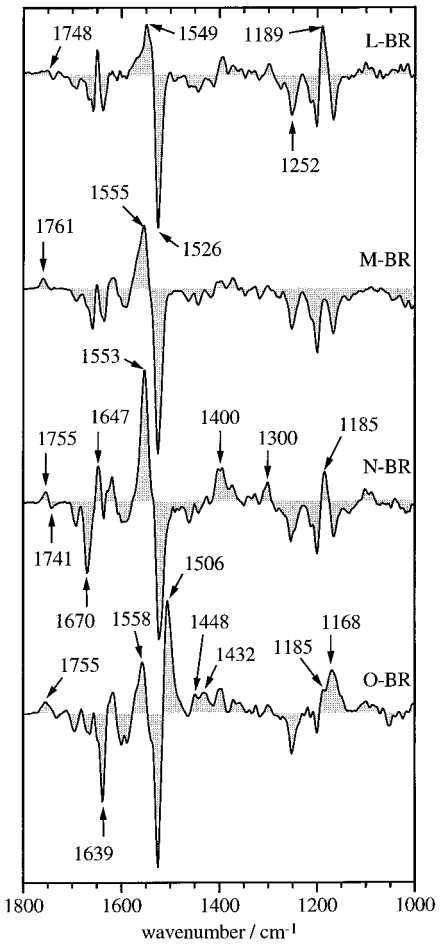

Figure 2. Difference spectra of L−BR (10 μs, pH 6.6, 20 °C), M−BR (300−400 μs, pH 8.4, 20 °C), N−BR (80−100 ms, pH 8.4, 20 °C), and O−BR (5−10 ms, pH 4.0, 40 °C). For clarity, spectra have been scaled to yield identical difference absorbance at 1252 cm^{-1}.

In Figure 2 difference spectra between the photointermediates L, M, N, and O (positive bands) and the unphotolyzed BR (negative bands) are displayed. Similar difference spectra recorded with the time-resolved transmission technique have already been reported.[13,21,22] Good agreement with the ATR spectra presented here can be found. Differences concerning the relative size of bands may originate from the different polarization conditions of the measuring light in transmission and ATR experiments.[15] Because these spectra have been discussed in detail in the literature, we are giving only a brief description of the most prominent features. The strongest band is located at 1526 cm^{-1} and has been assigned to the C═C double bond of retinal in the unphotolyzed state. The corresponding bands of the photoproducts are shifted to 1549 cm^{-1} in L, 1555 cm^{-1} in M, 1553 cm^{-1} in N, and 1506 cm^{-1} in O but are overlapped by amide II difference bands. The C−C single bonds of the chromophore are absorbing in the region between 1150 and 1280 cm^{-1}. The negative band at 1639 cm^{-1} has been attributed to the protonated Schiff base in the unphotolyzed state of BR.[23,24] It is of equal intensity in L and M, much smaller in N, and most pronounced in O. Other bands involving the Schiff base can be found around 1300 cm^{-1} (C−H in-plane vibration) and 1400 cm^{-1} (N−H in-plane).[11] They are strong in L and N.

Changes in secondary structure can be observed between 1500 and 1600 cm^{-1} (C═N−H, amide II) and between 1600 and 1700 cm^{-1} (C═O, amide I). They already show up in L and M, reach maximum intensity in N, and are mostly reversed in O.

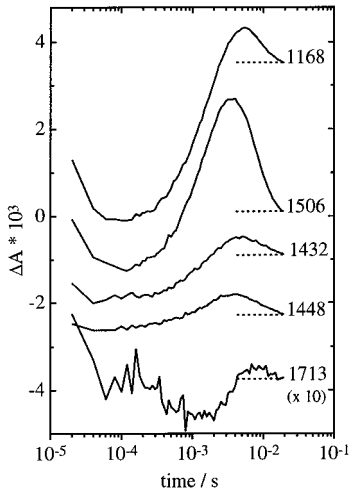

Figure 3. Time traces of bands typical for the O intermediate (wavenumbers as indicated). For clarity, traces are off-set and the time trace at 1713 cm^{-1} is magnified 10-fold. Experimental conditions are pH 4 and 40 °C.

TABLE 1: Band Assignment of the Wild-Type O−BR Difference Spectrum. Positive Bands (+) Correspond to the O Intermediate and Negative Bands (−) to the Ground-State BR

wavenumber/cm^{-1}	(tentative) assignment
1755 (+)	C═O of D85
1743 (+), 1733 (−)	C═O of D115
1713 (+)	C═O of unidentified D or E
1695 (−), 1671 (−), 1663 (−)	C═O of amide I
1639 (−), 1628 (+)	C═N−H of Schiff base
1558 (+)	C═N amide II
1526 (−), 1506 (+)	C═C stretch of retinal
1448 (+), 1432 (+)	CH_3 deformation of retinal
1168 (+)	C−C stretch of retinal

Bands above 1700 cm^{-1} are due to the C═O stretching vibration of protonated carboxylic acids coupled with the in-plane bending vibration of the O−H. The band at 1761 cm^{-1} in M has been assigned to the primary acceptor of the Schiff base proton, D85.[3] This band shifts to 1755 cm^{-1} in N, interpreted as a change of environment of D85.[25] It shows the same amplitude in the O−BR difference spectrum. Therefore, it can be concluded that D85 is still protonated in O. D96, which is the donor of the Schiff base proton, is protonated in the ground state and transiently deprotonated in N. The corresponding negative band in the N−BR difference spectrum is located at 1741 cm^{-1} [9].

The O Intermediate. Since the description of the O intermediate on a molecular level is a necessary requirement to understand the reset mechanism of the proton pump and the two infrared studies of the O intermediate in the literature are contradictory,[13,14] the O−BR difference spectrum (Figure 2 and Table 1) will be discussed in greater detail. Besides the characteristic bands at 1639, 1506, and 1168 cm^{-1} mentioned above, positive bands appear at 1432 and 1448 cm^{-1}. Corresponding frequencies in the preceding intermediates exhibit negative absorbance changes. A comparison of the kinetics at 1432 and 1448 cm^{-1} with those at 1506 and 1168 cm^{-1} (Figure 3) clearly shows that these bands belong to O. On the basis of the frequency we tentatively assign the bands at 1432 and 1448 cm^{-1} to antisymmetric deformation vibrations of the methyl groups of retinal. They might be a result of the conformationally distorted structure of all-trans retinal in the O intermediate.

In Figure 4 the O−BR difference spectra of wild-type and the mutant E204Q are compared, both in H_2O and D_2O. In addition, the corresponding difference spectrum of the E204T

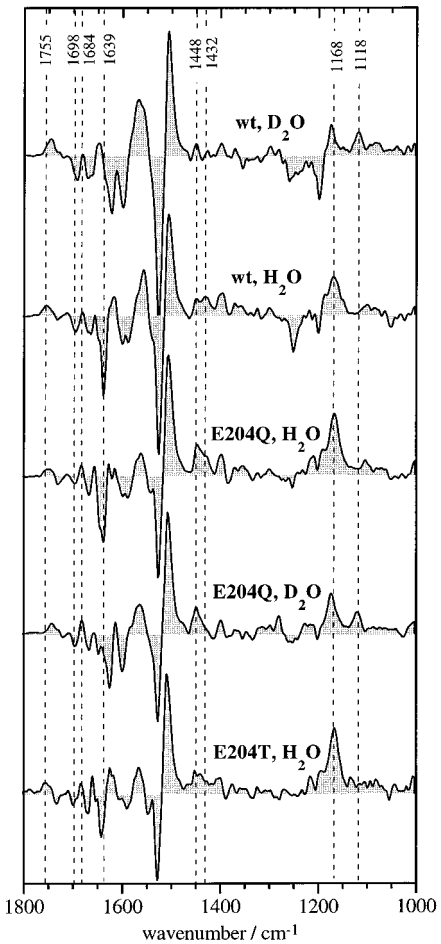

Figure 4. Comparison of O−BR difference spectra of wild-type BR in D_2O and H_2O, respectively, with those of the E204Q and the E204T mutant. Spectra were taken under the following conditions (from top to bottom): 10−20 ms, pD 4.4, 40 °C for wild-type BR in D_2O; 5−10 ms, pH 4.0, 40 °C for wild-type BR in H_2O; 100−220 ms, pH 4.0, 20 °C for the E204Q mutant in H_2O; 300−400 ms, pD 4.4, 20 °C for the E204Q mutant in D_2O; 30−120 ms, pH 4.0, 20 °C for the E204T mutant in H_2O. Difference spectra have been scaled to equal absorbancies at 1506 cm^{-1}. The second spectrum from top is reprinted from Figure 2.

mutant in H_2O is presented. Because the noise in the E204Q data is lower than in the E204T data, we focus on the E204Q mutant. The E204T difference spectrum is shown to confirm the results with E204Q. Compared to the wild-type, bands typical for O (1506, 1448, and 1168 cm^{-1}) are more pronounced in E204Q relative to bands of the unphotolyzed state. This is a consequence of the higher transient concentration of O in the mutant due to its slower decay compared to the wild-type (cf. Material and Methods section). Therefore, we have to conclude that there are, though very small, contributions of M and/or N in the wild-type O−BR difference spectrum. Accordingly, the positive amide II band at 1558 cm^{-1} is smaller in E204Q than in wild-type. However, the differences of wild-type and E204Q discussed below are only marginally affected by subtracting variable amounts of M−BR or N−BR difference spectra from the wild-type O−BR spectrum. Particularly, subtraction of other intermediates does not result in a negative band at 1698 cm^{-1} and/or a positive band at 1684 cm^{-1} as observed in the mutant spectrum. From the frequencies and the insensitivity to H/D exchange we assign these bands to amide I modes. We would like to point out that the band at 1698 cm^{-1} is located at almost the same frequency as the C═O vibration of E204 according to Brown et al.[6] (1700 cm^{-1}). Therefore, special care is necessary in analyzing this spectral region for protonation changes of E204.

The loss of difference absorbance between 1698 and 1684 cm^{-1} in the E204Q mutant can be ascribed to the lack of a negative difference band located around 1690 cm^{-1} that is insensitive to D_2O. It can be assigned to an amide I mode for the same reasons as the bands at 1698 and 1684 cm^{-1}. Thus, the band at 1695 cm^{-1} in the wild-type spectrum is a composition of several amide I modes. Mutation at position 204 influences some of these modes by inhibiting a minute change in secondary structure which normally occurs in wild-type. Another line of interpretation would involve a (protonated) arginine residue, presumably R82. Its possible interaction with E204 might be broken in the mutant. The lack of a substantial isotope downshift (∼50 cm^{-1})[26] contradicts this hypothesis. Around 1690 cm^{-1} C═O side chain vibrations of a glutamine or asparagine should also be considered. Yet, in the model of the BR structure based on electron diffraction data[27] there is no glutamine or asparagine in the vicinity of E204 to form a salt bridge. Spectral contributions of the C═O stretch of the side chain of Q204 can be ruled out by employing the E204T mutant, which exhibits the same band pattern (lowest spectrum in Figure 4).

On the basis of these results we suggest some correlations between amide bands and the location of secondary structure changes. The influence of the mutation of E204 on the band pattern around 1690 cm^{-1} might be related to changes of the protein backbone conformation close to E204 at the extracellular surface. The high frequency of this band favors its assignement to β-turns.[28,29] In the structural model of BR[27] a β-turn type I can be identified at the extracellular end of helix F. It includes S193 and E194 and is connected by a short loop with helix G, where E204 is located. The distance between E204 and S193 is very small, and E204 might interact directly with S193 or via the FG loop. E204 can also interact with E9 or residues of the BC loop, like E74 and Y79. However, the temperature factor of this area is high, indicating that the position of these residues is uncertain.

Comparing the difference spectra of Figure 4 reveales an additional band at 1118 cm^{-1} in D_2O both for wild-type BR and the E204Q mutant. The appearance of this band is accompanied by a loss of intensity at 1168 cm^{-1} with a slight shift of the band maximum toward higher wavenumbers. According to resonance Raman spectroscopy this band is due to coupling of the $C_{10}-C_{11}$ with the $C_{12}-C_{13}$ stretching vibration of retinal.[12] Although a band close to 1118 cm^{-1} is present in the resonance Raman spectrum of the O intermediate in D_2O, the origin of this band was not discussed.[12] The unphotolyzed state shows no analogous shift of a strong infrared band to 1118 cm^{-1} upon deuteration. Instead, a loss of intensity of the band at 1252 cm^{-1} accompanied by an increase in intensity at 1200 cm^{-1} is observed. Smith et al.[12] suggested that the band at 1252 cm^{-1} of the unphotolyzed state and the band at 1168 cm^{-1} of the unphotolyzed state and of O have remarkable contributions of the $C_{12}-C_{13}$ stretching vibration. Therefore, we conclude that the $C_{12}-C_{13}$ vibration is coupled to the C═N−H vibration. This explains why only parts of the bands centered at 1168 and 1252 cm^{-1} are D_2O sensitive. The band at 1448 cm^{-1} is not affected by H/D exchange, but a decrease in intensity at 1432 cm^{-1} is observed.

Figure 5 depicts O−BR difference spectra in the carbonyl region of wild-type BR in H_2O and D_2O, respectively. As in N, the band of protonated D85 shifts upon deuteration from 1755 to 1745 cm^{-1}. The shoulder at 1743 cm^{-1} and the negative band at 1733 cm^{-1} are shifting 11 cm^{-1} toward lower frequencies in D_2O. Like other bands typical for O, they are more pronounced in the E204 mutants (Figure 4). These two bands

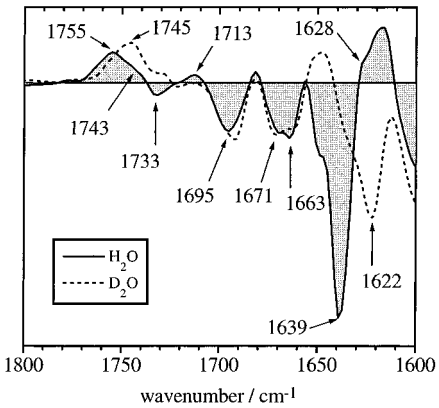

Figure 5. Carbonyl region of the wild-type O−BR difference spectra in H_2O (solid line, shaded) and D_2O (dashed line).

(1743 cm^{-1} +, 1733 cm^{-1} −) may originate from a change in the environment of a (protonated) carboxylic acid with a ground-state absorption at 1733 cm^{-1}. A good candidate for this frequency is D115.[30] At 1713 cm^{-1} a small positive band appears that is also detectable in the E204 mutants. In D_2O this band is obscured due to shifting into the adjacent amide I region. The positive absorbance change at 1713 cm^{-1} is interpreted to arise from the carbonyl vibration of a yet unknown aspartate or glutamate that is protonated during the lifetime of O (Figure 3). Within the framework of Govindjee et al.[31] this implies that the proton residing at D85 is not directly transferred to the extracellular medium during O decay. A consecutive intermediate state might be formed where another residue is protonated. However, a change in the vicinity of a protonated carboxylic acid resulting in a positive band at 1713 cm^{-1} cannot be strictly excluded.

From resonance Raman spectroscopy the C═N−H stretching mode of the Schiff base was assigned to bands at 1639 cm^{-1} for the ground state and at 1628 cm^{-1} for the O intermediate, respectively.[12] The 1639 cm^{-1} band is clearly observable in Figure 5, whereas the 1628 cm^{-1} band appears as a shoulder. The band of the unphotolyzed state is downshifted by 17 cm^{-1} to 1622 cm^{-1} in D_2O. According to the resonance Raman experiments, H/D exchange results in a downshift of the C═N−H vibration to 1589 cm^{-1}. In this area spectral overlap is strong and we cannot detect this band in our FT-IR difference spectra (Figure 4).

The bands at 1695, 1671, and 1663 cm^{-1} hardly shift upon deuteration. Thus, they are composed of mostly amide I vibrations reflecting changes in the secondary structure of the protein. It should be stressed that these changes are much smaller than the corresponding bands in the N−BR difference spectrum (Figure 2). In particular, bands at 1670 and 1647 cm^{-1} are strong in N but almost absent in M and O. The amide II band around 1553 cm^{-1} behaves in a similar way. Therefore, we conclude that the major structural changes observed in N are reversed during the transition to the O intermediate.

In previous time-resolved FT-IR studies, O−BR difference spectra have been obtained from the Y185F mutant[13] and by factor analysis of wild-type spectra.[14] Both of these studies claim that D85 and D96 are protonated in O, which is confirmed by our results. The O−BR difference spectrum of the Y185F mutant displays only minor changes in the amide I region, again in agreement with our studies.[32] In contrast, the spectrum calculated by factor analysis[14] shows large absorbance changes in the amide I region (1670 cm^{-1}) and a positive band at 1187 cm^{-1} which dominates the fingerprint region. These features are typical for the N intermediate and result most probably from imperfect separation by factor analysis of data gained under conditions where O contributes only minorly to the transient absorption changes (T = 25 °C, pH = 6.5). With resonance Raman spectroscopy, where chromophore bands are selectively monitored, the most prominent bands have been determined to be located at 1509, 1198, and 1168 cm^{-1} in the O intermediate.[12] A band at 1187 cm^{-1} was not reported but can be found in the resonance Raman spectrum of N.[33] This confirms that the O−BR difference spectrum presented in our study shows hardly any contamination with other intermediates, in contrast to the wild-type spectrum of ref 14. Possible contributions of the 13-cis photocycle of dark-adapted BR can be ruled out for the following reasons. It was demonstrated[34] that the amount of 13-cis retinal is constant over temperatures between 0 and 40 °C. However, the rate of dark adaption is accelerated at low pH, but still, it is on the order of several minutes at pH 4.[35,36] Since in our measurements the repetition frequency of the exciting laser was higher than 1 Hz at low pH, no significant amounts of 13-cis photoproducts are supposed to occur. Hence, inspection of L−BR difference spectra at various temperature and pH values[37] did not reveal any spectral features characteristic of 13-cis retinal. The slow photoproduct of 13-cis retinal BR has the electronic absorption maximum at 585 nm.[38] Correlating this maximum with the vibrational transition of the C═C stretching frequency[39] would result in a band around 1520 cm^{-1}. Yet, no such maximum or shoulder is detectable in the O−BR difference spectrum (Figure 2).

In conclusion, we demonstrate that with time-resolved ATR/FT-IR spectroscopy a clear-cut separation of the BR photointermediates is feasible. The focus on the O intermediate solves the controversy about alterations in secondary structure. We show that the major structural changes observed in the N intermediate at 1670 and 1647 cm^{-1} are reversed in the O intermediate.[40] Moreover, new bands of O are discovered and tentatively assigned. Applying the presented methodology to the pH dependence of the BR photoreaction allows the determination of transient pK_a changes of amino acid side chains.[37] This knowledge will be the basis of a detailed understanding of proton transfer in such inhomogeneous matrices as proteins.

Acknowledgment. We are indepted to Dr. G. Büldt for his continuous support and interest in this work. Dr. J. Granzin is acknowledged for advice in analyzing the BR structure, A. Cousin for the cultivation of the S9 strain of *Halobacterium salinarium* and isolation of purple membrane fragments, and R. Kofahl for technical assistance. We are grateful to Drs. D. Oesterhelt and J. Tittor (Max-Planck-Institut für Biochemie, Martinsried) for the generous gift of the E204Q and E204T mutants and for critical reading of the manuscript. This work was supported by a grant from the Deutsche Forschungsgemeinschaft (SFB 189/B15 to J.H.).

References and Notes

(1) Ebrey, T. G. In *Thermodynamics of Membranes, Receptors and Channels*; Jackson, M., Ed; CRC Press: Inc.: Boca Raton FL, 1993; p 353.

(2) Lanyi, J. K. *Biochim. Biophys. Acta* **1993**, *1183*, 241.

(3) Braiman, M. S.; Mogi, T.; Marti, T.; Stern, L. J.; Khorana, H. G.; Rothschild, K. J. *Biochemistry* **1988**, *27*, 8516.

(4) Heberle, J.; Dencher, N. A. *Proc. Natl. Acad. Sci. U.S.A.* **1992**, *89*, 5996.

(5) Scharnagl, C., Hettenkofer, J., Fischer, S. F. *J. Phys. Chem.* **1995**, *99*, 7787.

(6) Brown, L. S.; Sasaki, J.; Kandori, H.; Maeda, A.; Needleman, R.; Lanyi, J. K. *J. Biol. Chem.* **1995**, *270*, 27122.

(7) Butt, H. J.; Fendler, K.; Bamberg, E.; Tittor, J.; Oesterhelt, D. *EMBO J.* **1989**, *8*, 1657.

(8) Otto, H.; Marti, T.; Holz, M.; Mogi, T.; Lindau, M.; Khorana, H. G.; Heyn, M. P. *Proc. Natl. Acad. Sci. U.S.A.* **1989**, *86*, 9228.

(9) Gerwert, K.; Souvignier, G.; Hess, B. *Proc. Natl. Acad. Sci. U.S.A.* **1990**, *87*, 9774.
(10) Riesle, J.; Oesterhelt, D.; Dencher, N. A.; Heberle, J. *Biochemistry* **1996**, *35*, 6635.
(11) Maeda, A. *Isr. J. Chem.* **1995**, *35*, 387.
(12) Smith, S. O.; Pardoen, J. A.; Mulder, P. P. J.; Curry, B.; Lugtenburg, J.; Mathies, R. *Biochemistry* **1983**, *22*, 6141.
(13) Bousché, O.; Sonar, S.; Krebs, M. P.; Khorana, H. G.; Rothschild, K. J. *Photochem. Photobiol.* **1992**, *56*, 1085.
(14) Hessling, B.; Souvignier, G.; Gerwert, K. *Biophys. J.* **1993**, *65*, 1929.
(15) Heberle, J.; Zscherp, C. *Appl. Spectrosc.* **1996**, *50*, 588.
(16) Oesterhelt, D.; Stoeckenius, W. *Methods Enzymol.* **1974**, *31*, 667.
(17) Hofrichter, J.; Henry, E. R.; Sommer, J. H.; Deutsch, R.; Ikeda-Saito, M.; Yonetani, T.; Eaton, W. A. *Biochemistry* **1985**, *24*, 2667.
(18) Maurer, R.; Vogel, J.; Schneider, S. *Photochem. Photobiol.* **1987**, *46*, 247.
(19) The transient pH change along the purple membrane surface due to proton pumping by BR is smaller than 0.2 pH units in an unbuffered suspension (calculated from data of ref 4). The change in bulk medium pH is only 0.05. Although the ability of the used buffers to diffuse between the purple membrane sheets is not precisely known, the small pH change by proton pumping will be decreased by the buffer. This rules out any large effects on the photocycle kinetics. The chemical nature and the concentration of the buffers used do not influence the photoreaction (cf. ref 4).
(20) Mäntele, W; Siebert, F.; Kreutz, W. *FEBS Lett.* **1981**, *128*, 249.
(21) Chen, W.-G.; Braiman, M. S. *Photochem. Photobiol.* **1991**, *54*, 905.
(22) Weidlich, O.; Siebert, F. *Appl. Spectrosc.* **1993**, *47*, 1394.
(23) Lewis, A.; Spoonhower, J.; Bogomolni, R. A.; Lozier, R. H.; Stoeckenius, W. *Proc. Natl. Acad. Sci. U.S.A.* **1974**, *71*, 4462.
(24) Siebert, F.; Mäntele, W. *Eur. J. Biochem.* **1983**, *130*, 565.
(25) Braiman, M. S.; Bousché, O.; Rothschild, K. J. *Proc. Natl. Acad. Sci. U.S.A.* **1991**, *88*, 2388.
(26) Braiman, M. S.; Walter, T. J.; Briercheck, D. M. *Biochemistry* **1994**, *33*, 1629.
(27) Grigorieff, N.; Ceska, T. A.; Downing, K. H.; Baldwin, J. M.; Henderson, R. *J. Mol. Biol.* **1996**, *259*, 393.
(28) Bandekar, J; Krimm, S. *Proc. Natl. Acad. Sci. U.S.A.* **1979**, *76*, 774.
(29) Surewicz, W. K.; Mantsch, H. H. *Biochim. Biophys. Acta* **1988**, *952*, 115.
(30) Sasaki, J.; Lanyi, J. K.; Needleman, R.; Yoshizawa, T.; Maeda, A. *Biochemistry* **1994**, *33*, 3178.
(31) Govindjee, R.; Misra, S.; Balashov, S. P.; Ebrey, T. G.; Crouch, R. K.; Menick, D. R. *Biophys. J.* **1996**, *71*, 1011.
(32) It should be stressed at this point that due to different polarization conditions the ATR technique is more sensitive to changes in the amide I modes of α-helixes than transmission spectroscopy (cf. ref 15).
(33) Ames, J. B.; Mathies, R. A. *Biochemistry* **1990**, *29*, 7181.
(34) Scherrer, P.; Mathew, M. K.; Stoeckenius, W. *Biochemistry* **1989**, *28*, 829.
(35) Balashov, S. P.; Govindjee, J.; Kono, M.; Imasheva, E.; Lukashev, E.; Ebrey, T. G.; Crouch, R. K.; Menick, D. R.; Feng, Y. *Biochemistry* **1993**, *32*, 10331.
(36) Drachev, L. A.; Dracheva, S. V.; Kaulen, A. D. *FEBS Lett.* **1993**, *332*, 67.
(37) Zscherp, C.; Heberle, J. Manuscript in preparation.
(38) Gergely, C.; Ganea, C.; Váró, G. *Biophys. J.* **1994**, *67*, 855.
(39) Aton, B.; Doukas, A. G.; Callender, R. H.; Becher, B.; Ebrey, T. G. *Biochemistry* **1977,** *16*, 2995.
(40) Note added in proof: During preparation of the manuscript Kandori et al.[41] published O−BR difference spectra of E204 mutants. The close agreement of their spectra with those presented here (Figure 4) confirms our findings. Minor differences may be explained by using different techniques (ATR, transmission) and different measuring conditions (pH, temperature, time) and by the lower signal-to-noise ratio of the difference spectra of Kandori et al.
(41) Kandori, H.; Yamazaki, Y.; Hatanak, M.; Needleman, R.; Brown, L. S.; Richter, H.-T.; Lanyi, J. K.; Maeda, A. *Biochemistry* **1997**, *36*, 5134.